Laser Field Distribution Dependence on The Missing Holes of Photonic Crystal Fiber

Abdulghafoor Ibrahim Abdullah

ghaa4@yahoo.com
Department of Physics / College of Education
University of Mosul

الخلاصة

الهدف من هذه الدراسة هو بيان ارتباط توزيع مجال ضوء الليزر بعدد ال   فجوات الهوائية المفقودة في قلب الليف البلوري الفوتوني. لذلك فقد تم اقتراح ثلاث تراكيب للألياف البلورية الفوتونية، المعلمات الرئيسية لهذه   التراكيب جميعها متماثلة ؛ نصف قطر الفجوة الهوائ ية ٠.٤٦ مايكرون والمسافة بين مركزي اي فجوتين متجاورتين (حجم الخطوة) ٢.٣ مايكرون بينما عدد حلقات الفجوات الهوائية هي حلقة واحدة في كل ليف   من الألياف المقترحة . إن الاختلاف فقط في عدد ا لفجوات الهوائية المفقودة في مركز قلب الليف . في الليف الأول عدد الفجوات الهوائية المفقودة هي واحدة وفي الثاني ثلاث فجوات وفي الليف الثالث هناك أربع فجوات هوائية مفقودة في مركز قلب الليف.

مواصفات التراكيب المقترحة والتي تشمل معامل الانكسار الفعال، التشتت، خسائر الحصر وتوزيع المجال تم حسابها ومناقشتها . أشارت النتائج إلى أن زيادة عدد الفجوات الهوائية المفقودة في قلب الليف قللت من التغير في شكل التشتت ودفعت الطول   ألموجي عند التشتت الصفري باتجاه الأطوال الموجية الأطول إضافة إلى تقليل قيم خسائر الحصر ولمدى واسع من   الأطوال الموجية. كما بينت الدراسة أيضاً، ومن خلال توزيع المجال ، الى ان الليف المقترح ذو المساحة الأكبر يعمل بالنمط عال المرتبة.

Abstract

The aim of this study is to show the laser field distribution dependence on the number of missing holes in the core of the photonic crystal fiber, so that three different structure of photonic crystal fibers (PCFs) were proposed, the parameters of the proposed structures are identical; hole diameter d is 0.46 μm, pitch size Λ is 2.3 μm, while the number of the hole rings (Nr) is one for all the structures. The difference only in the number of the missing holes in the center of the core, that means PCF1 of one missing holes, PCF2 of three missing holes, and PCF3 of four missing holes.

The characteristics of the PCFs structures such as effective index, dispersion, confinement losses and field distribution were calculated and discussed. The results of such study show that the increasing of the missing holes reduces the fluctuation in dispersion profile and pushing the zero dispersion wavelength (ZDW) towards the longer wavelength, in addition the confinement losses are reduced over a wide range of wavelength. This study shows, by the field distribution, that the PCFs of large core area are operated in high order mode.

1. Introduction

Photonic crystal fibers (PCFs) are a type of optical fibers, which are made from single material such as silica glass (SiO_2), with an array of microscopic air channels running along its length [1,2].

PCFs based on index-guiding, are formed by a defect, which can be created by filling one central air hole with glass (to form a core). The light is guided by total internal reflection (TIR) between the solid core and the cladding region. The cladding region is an array of air holes in regular triangular lattice as shown in Fig.1 [1,2].

In the past few years, the research of PCFs have been the subject of many group; Knight *et al* [1,2], Saitoh *et al* [3-8], Ferrando *et al* [9-11], Mortensen *et al* [12-14] and Kuhlmy *et al* [15,16], because PCFs offer design flexibility in controlling the dispersion profile.

PCFs have some unusual properties (which is not available in conventional fiber) such as endlessly single mode [1,6,13], flattened dispersion over a range of wavelength [7,11], ultra flattened with low confinement losses [5,15] nearly zero dispersion wavelength [10], zero dispersion at visible region [8], and very high negative dispersion [17]. These characteristics of PCFs make them useful candidate for Dense Wavelength Division Multiplexing (DWDM) and dispersion compensation applications [18]. All the properties mentioned above can be controlled by

manipulating the main parameters of the PCFs, such as air hole diameter d, pitch size Λ, number of the rings Nr, and number of missing holes MNr.

Various groups have modeled PCFs by different numerical tools [3,4, 7,9,15-18] for determining the waveguide parameters for light wave propagation in PCFs. Multipole method are one of them and is used to calculate the effective index (n_{eff}) of the infinite periodic photonic crystal cladding [15,16,19].

The aim of this study is to show how the numbers of missing holes influence on the properties of the PCF, such properties are effective index, dispersion, confinement loss and laser field distribution across the proposed PCFs at the communication windows 1.3 µm and 1.55 µm. On the other hand we focus our attention on negative dispersion at 0.8µm wavelength window of Ti-Za laser and even on flattened dispersion at communication windows of 1.3 µm and 1.55µm wavelength of semiconductor laser.
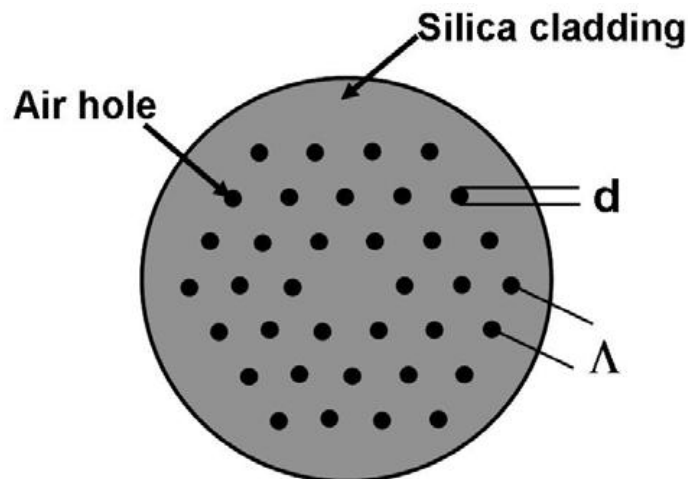

Fig. 1: A cross section diagram of a photonic crystal fiber.

2. Proposed photonic crystal fiber geometry and used software

Three PCFs structures have been considered in this paper consist of a pure silica with refractive index 1.4632264867 at λ = 0.5µm. The air holes of diameter (d= 0.46 µm) are arranged on an hexagonal form with pitch size (Λ=2.3 µm).

For PCF1, in the center one air hole is missed (MNr=1) creating a central high index defect serving as the core of the fiber. The number of the rings is (Nr=1) that means the number of the air holes in this structure is (NH=6).

For PCF2, same values of d, Λ, and Nr as in PCF1 were considered, while the number of missing holes (MNr=3), therefore the number of holes in the PCF2 structure are (NH=18).

For PCF3, (also) the same values of d, Λ, and Nr as in PCF1 were considered, while the number of missing holes (MNr=4), therefore the number of holes in the PCF structure are (NH=24). That means the continuous increase in the number of missing holes means increasing in the number of the holes in the clad.

The core radius R_c of the PCFs is calculated by the following relation:

$R_c = Nr \times Λ - d/2$ **1**

The cross section of the proposed PCFs structure shown in Fig.2, depending on the dimension of the proposed structures, the relative air hole size is d/Λ < 0.4 for PCF1, PCF2 and PCF3, that means the parameters of the proposed structures, at the beginning, are located in endlessly single mode as shown in Fig .3,[12].

| PCF1(MNr=1) | PCF2 (MNr=3) | PCF3(MNr=4) |
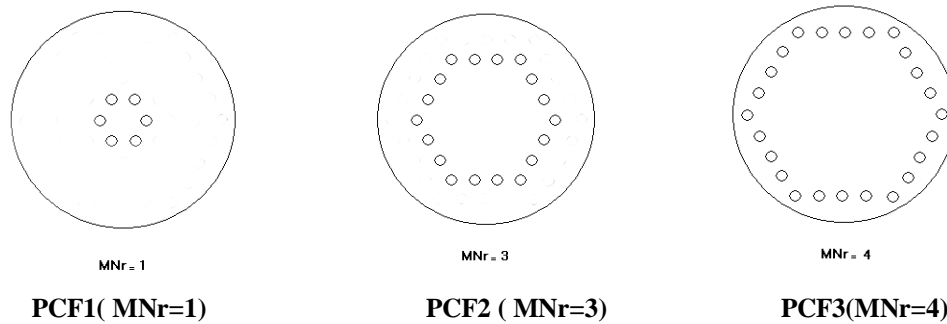
Fig. 2: Cross section of the proposed structure with core radius $R_c = Nr \times Λ - d/2$
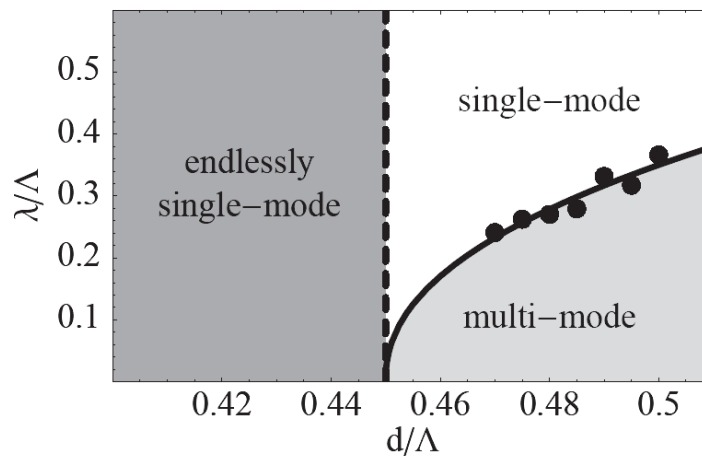
Fig.3. Cut-off phase diagram, the solid line separating the single and multi mode regimes for a fiber of one missing hole [12].

Numerical simulations which is based on the multipole method, as used by Kuhlmey *et al* [16] and White *et al* [19], to determine the effective indices of the proposed PCFs structures. The presented results are a combination of data from a program written by the author of this paper and from the CUDOS UTILITIES Software [20]. The software is created and distributed by the University of Sydney. The precision of the calculated mode indices have been found by an amount 1×10^{-11} for the real part [20] and for an imaginary part of the index is found by 1×10^{-15} [16].

3. Results and Discussion

Fig.4 shows the relation between the real part of the refractive index with wavelength for the proposed PCFs. The calculation have been done by using PCF1, PCF2 and PCF3 parameters.

The effective index is composed of the material part $n_{eff,mat.}$ and the geometric part $n_{eff,geom.}$ i.e:

$$n_{eff.} = n_{eff,mat} + n_{eff,geom.} \qquad \qquad 2$$

for a given material, only the geometrical part can be influenced.

It is evident from the figure that there is a significant difference in the real part of the effective refractive index, such difference due to the change in the missing holes. The figure shows that the increasing in the missing hole cause decreasing in the difference between the refractive index of the silica and the refractive index of the PCF1 for the fundamental mode comparing to the refractive index of both PCF2 of three missing holes and PCF3 of four missing holes.

Fig.4 shows also that the real part of the refractive index at shorter wavelength is approaching the core index, while for long wavelength is significantly below the core index.
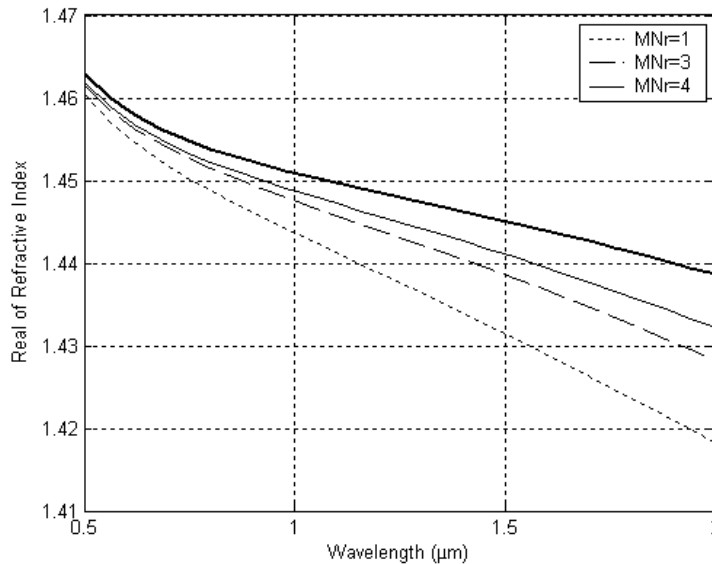
Fig. 4: Real part of the refractive index of the fundamental mode as a function of wavelength for the proposed structures, the bold line for silica.

Fig.5 shows the relation between the imaginary part of the refractive index as a function of wavelength. We found from this figure for PCF1 of MNr=1 the imaginary part of the refractive index is increased exponentially with increasing the wavelength. On the other hand PCF3 of MNr= 4 has lower imaginary part comparing with PCF1 &PCF2.
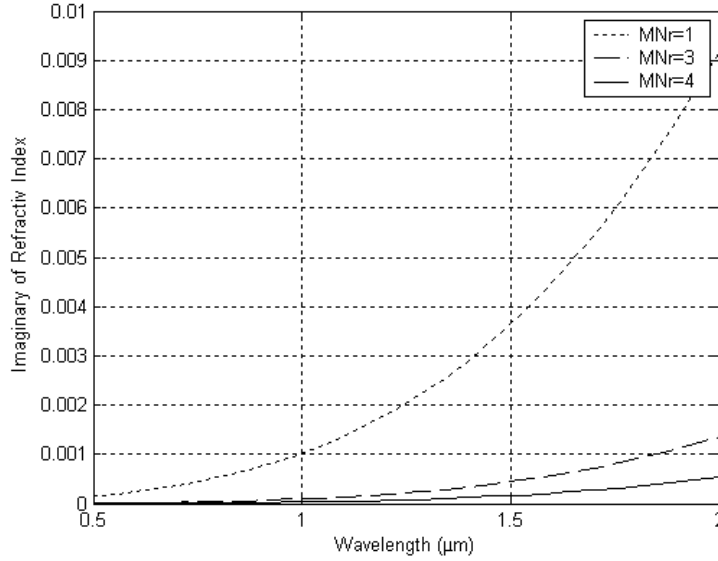
Fig. 5: Imaginary part of the effective index of the fundamental mode as a function of wavelength for the proposed structures.

4. Dispersion D(λ)

The result of this paper shows the dispersion property only when the variation in the number of missing holes MNr in the core of the PCFs is considered, while the other parameters (d, and Nr) are held constant. The chromatic dispersion D(λ) of a PCFs is calculated from the real value of the n_{eff} as a function of the wavelength using [11,15]:

$$D(\lambda)=(-\lambda/c)(d^2 \Re(n_{eff}) /d\lambda^2) \qquad\qquad\qquad\textbf{3}$$

where c is the velocity of the light in vacuum and $\Re$ stands for the real part of the effective index. The material dispersion is directly included in the calculation. According to Eq.3, the chromatic dispersion is calculated from the second derivative of the effective index with respect to wavelength.

Fig.6 shows that the increasing of the missing hole (means increasing the number of the holes in the clad) reduces the fluctuation in dispersion profile resulting near flat dispersion ~20ps/nm/km over a range of wavelength (1.1 to 1.65µm). This is very useful in wave division multiplexing technique. On the other hand, zero dispersion wavelength (ZDW) was pushed towards

longer wavelength (red shift at region 1.0 to 1.3µm). It is believed that due to increasing in the number of missing holes as shown by the figure inside. The values of the ZDW for the proposed structures are listed in table (1). Furthermore, this figure shows also that all the proposal structures have anomalous dispersion around -80 to -100ps/nm/km at communication wavelength 0.8µm of Ti-Za laser. These characteristics of the proposal PCFs make them useful candidate for Dense WDM [4] and dispersion compensation application [8], wide band super continuum generation and ultra short soliton transmission [18].
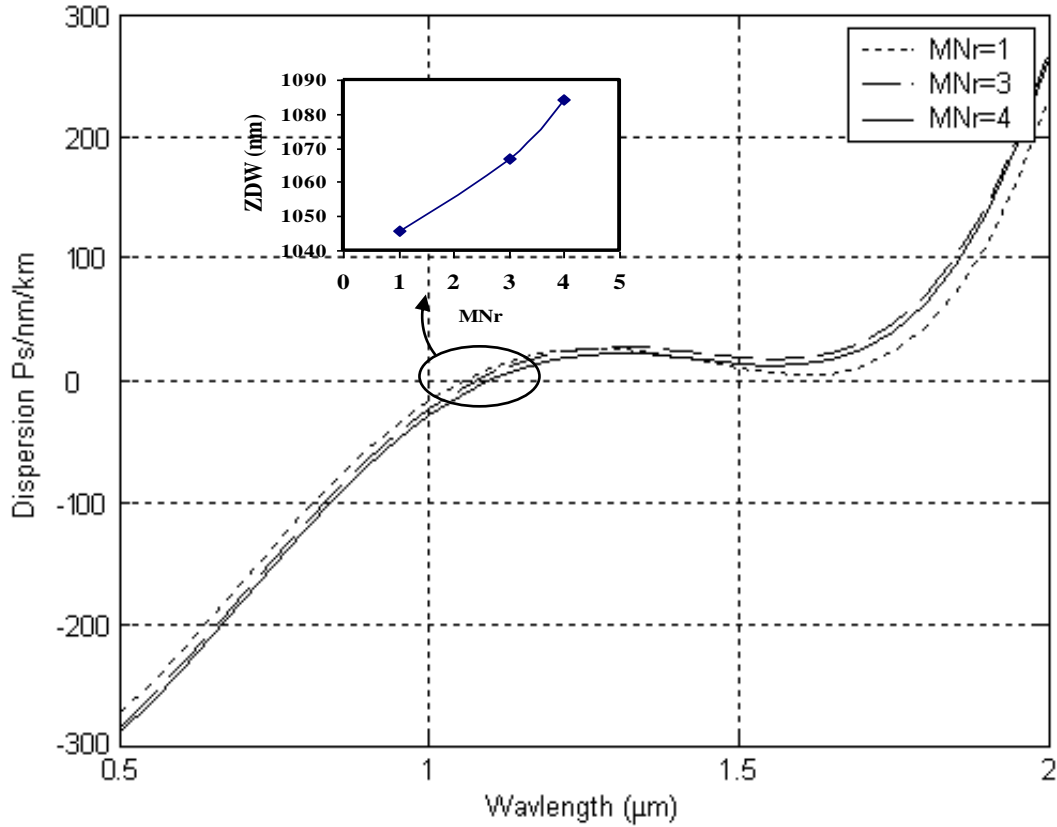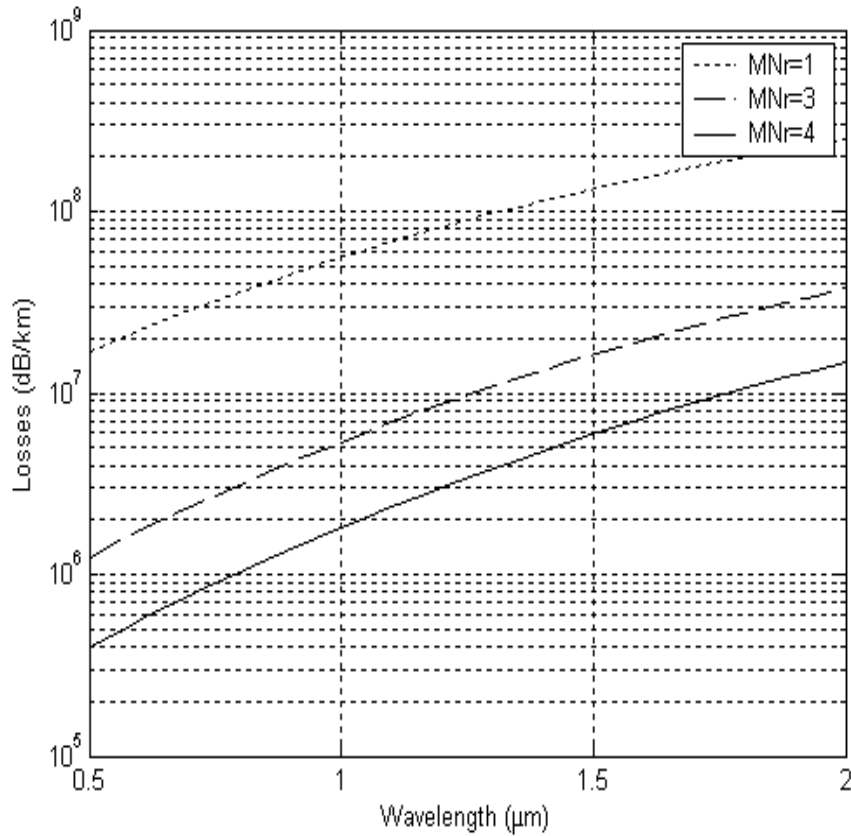

Fig.6. Computed dispersion as a function of wavelengths for a proposed PCFs.

Fig. 7: Computed confinement losses as a function of wavelengths for proposed PCFs.

5. Confinement losses

Fig. 7 shows the computed confinement losses values $L(\lambda)$, as a function of wavelengths for the fundamental mode of solid core PCFs which is calculated by the following relation [19]:

$$L(\lambda) = [40\pi/\lambda \ln(10)]Im(n_{eff}) \times 10^9 \qquad\qquad 4$$

Where λ, in micrometer, $L(\lambda)$ in dB/km and Im, stands for the imaginary part.

It is very clear that the guidance become better for PCF3 of four missing holes comparing to PCF1 and PCF2 of one missing hole and three missing holes respectively. In other words as the core radius increases (using Eq. 1) the confinement losses decreases. Therefore PCF3 of larger core area $252.64\mu m^2$ has lower confinement losses over a wide range of wavelength ($0.5\mu m$ to $2.0\mu m$). On the other hand the four missing holes pushing the confinement losses many times lower over a wide range of

wavelength. The less losses due to the increase of core area so one can say PCF3 is favorable for lower losses which are needed for some particular application like nonlinear effects.

The result can be explained phenomenological as follows. According to Fig.4 the real part of the effective refractive index for the PCF3 tends to be the real part of the effective refractive index for the silica. That means the propagation becomes increasingly parallel to the fiber axis, so the interaction with the confining structure is reduced [7].

6. Field distribution of the mode

Fig.9 shows the field distribution of the guided mode studied in this paper for MNr =1,3,4 at two communication wavelength 1.3 µm and 1.55 µm. It is clear that the light can be guided in the core with different profiles depends on the fiber structure, core area and the communication wavelength.

For PCF1 with one ring of six air holes, d=0.46 µm, Λ=2.3 µm, the relative air hole size is $d/\Lambda = 0.2$ and the relative wavelength λ/Λ =0.56 and 0.67 at 1.3µm 1.55µm communication wavelength respectively. The laser field distribution in the PCFs becomes more concentrated in the core region (A= 13.45µm^2) and avoids the holes compared with the same structure but with longer wavelength 1.55µm. Furthermore, this figure shows that the field distribution in PCF1 looks exactly the same as HE$_{11}$ mode, (the fundamental guided mode) in step index fiber and we can label it by the degenerate of HE$_{11}$ mode [22], that means the fiber is still operated in single mode regime.

For PCF2 with one ring of 18 air holes and PCF3 with one ring of 24 holes both structure of same relative air hole size is $d/\Lambda = 0.2$ but their core areas are 139.69 µm^2 and 252.64µm^2 respectively, means the core area is increased, the laser field distribution is extended more in the silica. The field is well confined in the core and there are almost no overlaps with cladding air holes. It is very clear from Fig.8 that the increase in the number of missing holes reduces the range of single mode operation and according to the dimensions of the PCF2 and PCF3 these structures lie in the region of the multimode operation as mentioned in Fig.8. Table (1), shows the summarized results obtained in the present work.

Table 1: Summary of the results

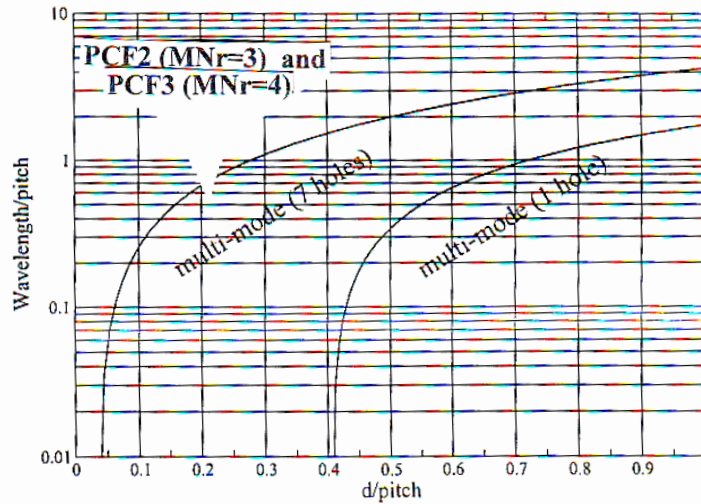| Parameters	PCF1	PCF2	PCF3	Units
Dispersion @800nm	90	95	100	
@ 1300nm	22	20	18	
@1550nm	10	20	15	ps/nm/km
Anomalous dispersion @800nm	-80	-95	-100	
Confinement losses @800nm	$3.0x10^7$	$3.0x10^6$	$1.0x10^6$	
@ 1300nm	$1.0x10^8$	$0.2x10^8$	$3.0x10^6$	dB/km
@1550nm	$0.5x10^9$	$1.1x10^7$	$8.0x10^6$	
ZDW	1.046	1.067	1.084	μm
Core area	13.45	193.69	252.64	$μm^2$

Fig. 8: Cut-off phase diagram for one and seven holes missing [21].

6. Conclusion

The main parameters (dispersion, anomalous dispersion, confinement losses, ZDW and core area at three wavelengths of communications) are shown in table (1). We could conclude from these results that all the structures have lower dispersion at window 1.3 μm, while PCF3 has higher anomalous dispersion at window 0.8 μm. In addition the confinement loss for PCF3 at window 0.8 μm is more distinguished than other fibers.

PCF of large area core can be used for providing high power delivery for application in astronomy and material processing.
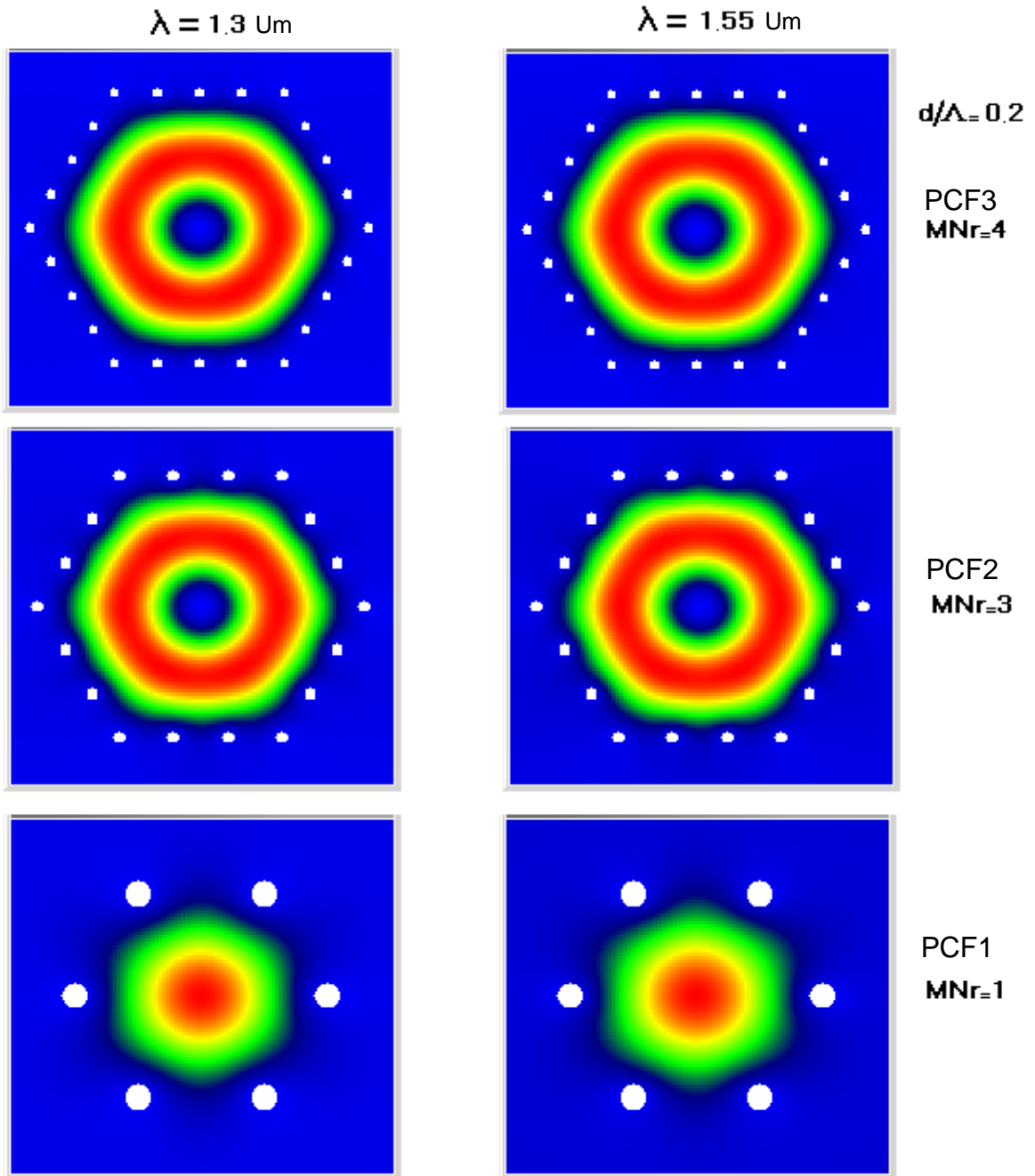
Fig. 9: The field distribution of the mode at communication wavelengths 1.3 & 1.55µm, all the proposed structures of relative air hole d/Λ = 0.2

REFERENCES

1) Knight J. C., Birks T. A., Russell P. St. J., and Atkin D. M., Opt. Lett., 21:1547- 1549 (1997).

2) Knight J. C., and Russell P. St. J., Science, 296: 267-277 (2002).

3) Saitoh K., and Koshiba M., IEEE J. Quant. Elect., 38:927-933 (2002).

4) Saitoh K., Koshiba M., Hasegawa T. and Sasaoka E., Opt. Exp., 11: 843-852 (2003).

5) Saitoh K., Florous N., and Koshiba M., "Opt. Exp., 13:8365-8371, (2005).

6) Saitoh K., Tsuchida Y., and Koshiba M., Opt. Soc. Am. (2005).

7) Saitoh K., and Koshiba M., Journal of light wave technology, 23:3580-3590 (2005).

8) Saitoh K., Koshiba M., and Mortensen N. A., New J. Phys. 8:1-9 (2006).

9) Ferrrando A., Silvestre E., Miret J. J., Andres M. V., and Andres P., Opt. Lett., 24:276-78 (1999).

10) Ferrrando A., Silvestre E., Miret J. J., and Andres P., Opt. Lett.,25:790-792 (2000).

11) Ferrrando A., Silvestre E., Andres P., Miret J. J., and Andres M. V., Opt. Lett., 9:687-697 (2001).

12) Mortensen N. A., Opt. Exp. 10:341-348 (2002).

13) Mortensen N. A., Folkenberg J. R., Skovgaard P. M. W. and Broeng J. IEEE Phot. Tech. Lett.: preprint, http://arxiv.org/abs/physics/0202073 (2002).

14) Mortensen N. A., Folkenberg J. R., Skovgaard P. M. W., Nielsen M. D., and Hansen P. K., Opt. Lett. 28:1879-1883 (2003).

15) Kuhlmey B. T., White T. P., Renversez G., Maystre D., Botten L. C., Sterek C. M. and McPhedran R. C., J. Opt. Soc. Am.B.19:2331-2340 (2002).

16) Kuhlmey B. T., McPhedran R. C., Sterek C. M., Robinson P. A., Renversez G., and Maystre D., Opt. Exp. 10:1285-1290 (2002).

17) Sinha R. K., and Varshney A. D., Opt. and Quant. Elect. 37:711-722 (2005).

18) Varshney S. K. and Sinha R. K., J. Micro. And Opto., 2:32-42(2002).

19) White T. P., Kuhlmey B. T., McPhedran R. C., Maystre D., Renversez G., Sterek C. M., and Botten L. C., J. Opt. Soc. Am.B.19:2322-2330 (2002).

20) CUDOS MOF UTILITIES Software ©Commonwealth of Australia 2004. http://www.physics.usyd.edu.au/cudos/mofsoftware/.

21) Blatting P., Romano V., Luthy W., and Feurer T., IAP Technical report (2006).

22) Guobin R., Zhi W., Shugin L., and Shuisheng J., Opt. Exp.Vol.11,No 11, 1310-1321,2003.